1. I.J. UWANTA, 2. M.M. HAMZA

UNSTEADY/STEADY FLOW OF VISCOUS REACTIVE, HEAT GENERATION/ABSORBING FLUID WITH SORET, DUFOUR AND VARIABLE VISCOSITY EFFECTS

1. Department of Mathematics, Usmanu Danfodiyo University, Sokoto, P.M.B. 2346, NIGERIA

Abstract: This study investigates the unsteady/steady natural convection and mass transfer flow of viscous reactive, heat generating/absorbing fluid in the presence of thermal diffusion, diffusion-thermo and temperature dependent variable viscosity in a vertical channel formed by two infinite parallel plates. The motion of the fluid is induced due to natural convection caused by the reactive property as well as the heat generating/absorbing nature of the fluid. The nonlinear governing equations are solved numerically using unconditionally stable and convergent semi-implicit finite difference scheme. Results of the computations for velocity, temperature, concentration, skin friction, rate of heat and mass transfer are presented graphically and discussed quantitatively for various controlling parameters embedded in the problem.
Keywords: Soret, Dufour, heat generation/absorbing, variable viscosity, reactive fluid

1. INTRODUCTION

Heat and mass transfer processes by natural convection in the presence of chemical reaction is important in many chemical engineering and petroleum chemical industries. Examples of such area of applications include tubular laboratory reactors, chemical vapor deposition systems, the oxidation of solid materials in large containers, the synthesis of ceramic materials by a self-propagating reaction, combustion in underground reservoirs for enhanced oil recovery and the reduction of hazardous combustion product using catalytic porous beds and many others. Campbell et al [1] concluded that the transport of heat and mass transfer within the reactors is controlled by diffusion or natural convection. When heat and mass transfer occur concurrently between the fluxes, the deriving potentials are of more complicated nature. Mass flux produced by a temperature gradient is refers to thermal diffusion (Soret effect) and heat flux generated by a concentration gradient is term as diffusion-thermo (Dufour effect). The Soret effect has been utilized for isotope separation, and in mixture between gases with very light molecular weight (He, H_2) and of medium molecular weight (N_2, air). The Dufour effect was found to be of considerable magnitude such that it cannot be neglected [2]. Many outstanding studies have considered combined thermal diffusion and diffusion-thermo effects in natural convection and mass transfer flow. Sparrow et al [3] studied the effects of Soret and Dufour for helium-air boundary layer in stagnation flow. Combined effects of Soret and Dufour on steady mixed convection flow are to be found in Hayat et al [4], and Alam and Rahman [5]. Cheng [6] analyzed the effects of Soret and Dufour over a vertical cone in a porous medium. In nutshell, there has been considerable published work dealing with steady flow with Soret and Dufour effect, some of them are Tsai and Huang [7, 8], Eugen and Postelnicu [9], Postelnicu [10], Shyam et al [11], Olanrewaju et al [12], Reddy and Reddy [13], Afify [14], Mahdy [15], Osalusi et al [16], Alam et al [17], and Chamkha and Ben-Nakhi [18]. Steady flows with chemical reaction considering Soret and Dufour effect are to be found in Postelnicu [19], Mansour et al [20], Beg et al [21], El-Kabeir et al [22], and

Gangadhar [23]. Unsteady flow problems in the presence of Soret and Dufour effects with chemical reaction can be found in Bhargava et al [24], and Pal and Mondal [25]. Vempati and Laxmi-Narayana-Gari [26] investigated Soret and Dufour effects on MHD flow in a vertical porous plate. Recently Al-Odat and Al-Ghamdi [27] examined numerically the effects of Soret and Dufour on unsteady MHD natural convection flow in a non-Darcy porous medium.

All the above-mentioned studies, assumed the viscosity of the fluid to be constant. However, it is known that the fluid physical properties may change significantly with temperature changes. To accurately predict flow behavior and heat transfer rate it is necessary to take into account the variation of viscosity with temperature Hossain et al [28]. In this direction, Kafoussias and Willians [29], Seddeek [30], and Moorthy and Senthilvadivu [31] studied the effects of thermal diffusion and diffusion-thermo in the presence of temperature dependent variable viscosity. On the other hand, the study of heat generation/absorption effects is also important in view of several physical problems, such as fluids undergoing endothermic or exothermic chemical reactions, fire and combustion modelling, and the development of metal waste from nuclear fuel. All the features for heat generating/absorbing fluids has been reported by Jha and Ajibade [32] in their studies on the free convective flow between vertical porous plates with periodic input. Abdullah [33] analyzed analytically heat and mass transfer over a permeable stretching plate affected by chemical reaction, internal heating, Dufour-Soret effect and Hall Effect.

Majority of the above-mentioned studies focused on steady flow and considered first order homogeneous chemical reaction. In this paper, an exothermic chemical reaction of Arrhenius kinetic is employed in the investigation of unsteady as well as steady flow of viscous reactive, heat generating/absorbing fluid in the presence of thermal diffusion, diffusion-thermo and temperature dependent variable viscosity in a channel formed by two infinite vertical parallel plates.

2. MATHEMATICAL ANALYSIS

Consider the unsteady natural convection and mass transfer flow of viscous reactive, heat generating/absorbing fluid between two infinite vertical parallel plates (see fig.1). The convective current is as a result of the reactive property of the fluid as well as heat generating/absorbing nature of the fluid. Initially, it is assumed that both the fluid and the plates are at rest and at same temperature and concentration $T_0^{'}$ and $C_0^{'}$ respectively. At time $t' > 0$ the temperature and concentration of the plate $y' = 0$ is raised to $T_{\omega}^{'}$ and $C_{\omega}^{'}$, and thereafter remains constant and that of $y' = H$ is lowered to $T_0^{'}$ and $C_0^{'}$, where $T_{\omega}^{'} > T_0^{'}$ and $C_{\omega}^{'} > C_0^{'}$. The Soret and Dufour effects are taken into account. The fluid temperature dependent variable viscosity is of type given by Kafoussias and Willians [29] $\overline{\mu} = \dfrac{\mu_0}{\left[1 + \gamma\left(T' - T_0^{'}\right)\right]}$, where μ_0 is the initial fluid dynamic viscosity at the temperature, $T_0^{'}$. Under these assumptions along with the Boussinesq's approximation, the governing equations can be written as

$$\frac{\partial u'}{\partial t'} = \frac{\partial}{\partial y'}\left(\overline{\mu}\frac{\partial u'}{\partial y'}\right) + g\beta(T' - T_0^{'}) + g\beta^*(T' - T_0^{'}) \tag{1}$$

$$\frac{\partial C'}{\partial t'} = D_m\frac{\partial^2 C'}{\partial y'^2} + \frac{D_m k_T}{T_m}\frac{\partial^2 T'}{\partial y'^2} \tag{2}$$

$$\frac{\partial T'}{\partial t'} = \frac{k}{\rho C_p}\frac{\partial^2 u'}{\partial y'^2} + \frac{QC_0^* A}{\rho C_p}e^{\left(\frac{-E}{RT'}\right)} + \frac{D_m k_T}{c_s C_p}\frac{\partial^2 C'}{\partial y'^2} + \frac{Q_0\left(T_0^{'} - T'\right)}{\rho C_p} \tag{3}$$

The initial and boundary conditions for the present problem are

$$\left. \begin{array}{l} t' \le 0 : u' = 0, \ T' \to T_0^{'}, \ C' \to C_0^{'}, \ 0 \le y' \le H \\ t' > 0 : u' = 0, T' = T_{\omega}^{'}, \ C' = C_{\omega}^{'} \ at \quad\quad y' = 0 \\ \quad\quad u' = 0, \ T' = T_0^{'}, \ C' = C_0^{'} \ as \quad\quad y' \to H \end{array} \right\} \tag{4}$$
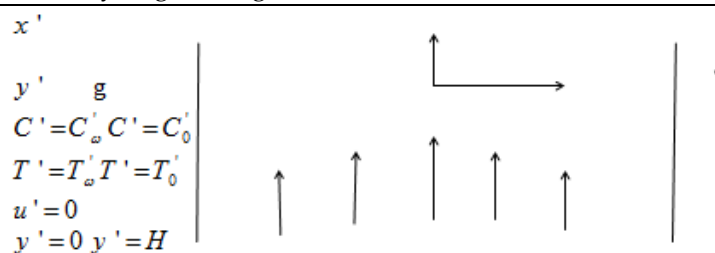
Fig.1. Schematic diagram of the physical model and coordinate system

where β is the coefficient of thermal expansion, β^* is the coefficient of concentration expansion, Q is the heat of reaction, Q_0 is the dimensional heat generating/absorbing fluid parameter, A is the rate constant, E is the activation energy, R is the universal gas constant, v is the kinematic viscosity, C_0^* is the initial concentration of the reactant species, g is the gravitational force, C_p is the specific heat at constant pressure, k is the thermal conductivity of the fluid, ρ is the density of the fluid, D_m is the coefficient of mass diffusivity, T_m is the mean fluid temperature, k_T is the thermal diffusion ratio and c_s is the concentration susceptibility.

To solve equations (1) to (4), we employ the following dimensionless variables and parameters

$$
\left.
\begin{array}{l}
y = \dfrac{y'}{H}, \quad t = \dfrac{t'\mu_0}{H^2}, \quad U = \dfrac{u'}{\mu_0}, \quad \Pr = \dfrac{\mu_0 \rho C_p}{k}, \quad Gc = \dfrac{g\beta^* RC_0^2 H^2}{E\mu_0^2}, Gr = \dfrac{g\beta RT_0^2 H^2}{E\mu_0^2} \\[3mm]
\theta = \dfrac{E(T'-T_0)}{RT_0^2}, \quad \lambda = \dfrac{QC_0^* AEH^2}{RT_0^2}e^{\left(\frac{-E}{RT_0}\right)}, \quad Sc = \dfrac{v}{D_m}, \quad Sr = \dfrac{k_T T_0^2}{T_m C_0^2}, \quad C = \dfrac{E(C'-C_0)}{RC_0^2} \\[3mm]
\varepsilon = \dfrac{RT_0}{E}, \theta_a = \dfrac{E(T_\omega - T_0)}{RT_0^2}, C_a = \dfrac{E(C_\omega - C_0)}{RC_0^2}, S = \dfrac{Q_0 H^2}{k}, Du = \dfrac{D_m k_T C_0^2}{\mu_0 c_s C_\rho T_0^2}, X = \dfrac{bRT_0^2}{E}
\end{array}
\right\}
\tag{5}
$$

Using (5), the equations (1) to (5) take the following form:

$$
\frac{\partial U}{\partial t} = \frac{\partial}{\partial y}\left((1-X\theta)\frac{\partial U}{\partial y}\right) + Gr\theta + GcC
\tag{6}
$$

$$
Sc\frac{\partial C}{\partial t} = \frac{\partial^2 C}{\partial y^2} + Sr\frac{\partial^2 \theta}{\partial y^2}
\tag{7}
$$

$$
\frac{\partial \theta}{\partial t} = \frac{1}{\Pr}\frac{\partial^2 \theta}{\partial y^2} + \frac{\lambda}{\Pr}e^{\left(\frac{\theta}{1+\varepsilon\theta}\right)} - \frac{S\theta}{\Pr} + Du\frac{\partial^2 C}{\partial y^2}
\tag{8}
$$

The initial and boundary conditions in dimensionless form are

$$
\left.
\begin{array}{l}
u = 0, \ \theta = 0, \quad 0 \le y \le 1, t \le 0 \\
t > 0 : u = 0, \ \theta = \theta_a, C = C_a \ at \ y = 0 \\
u = 0, \theta = 0, \ C = 0, \ as \ y = 1
\end{array}
\right\}
\tag{9}
$$

where X, Gr, Gc, S, Sc, Sr, Pr, λ, ε, Du, θ_a, and C_a are variable viscosity parameter, thermal Grashof number, mass Grashof number, heat generating/absorbing parameter, Schmidt number, Soret number, Prandtl number, Frank-Kamenetskii parameter, activation energy parameter, Dufour number, ambient temperature, and ambient concentration respectively. The other non-dimensional quantities are the skin friction (C_f), the heat transfer rate (Nu), and the rate of mass transfer (Sh) given as

$C_f = \dfrac{\partial U}{\partial y}\bigg|_{y=0,1}$, $Nu = -\dfrac{\partial \theta}{\partial y}\bigg|_{y=0,1}$, $Sh = -\dfrac{\partial C}{\partial y}\bigg|_{y=0,1}$, where C_f is the skin friction, Nu is the Nusselt

number and Sh is the Sherwood number.

3. NUMERICAL SOLUTIONS

The non-dimensional governing equations (6) to (8) with the boundary conditions (9) are solved numerically using semi-implicit finite difference scheme given in [34]. We used forward difference formulas for all time derivatives and approximate both the second and first derivatives with

second order central differences. The semi-implicit finite difference equation corresponding to equations (6) to (8) are as follows

$$-r_1\mu U_{j-1}^{(N+1)} + (1+2r\mu_1)U_j^{(N+1)} - r_1\mu U_{j+1}^{(N+1)} = r_2\mu U_{j-1}^{(N)} + (1-2r_2\mu)U_j^{(N)} + r_2\mu U_{j+1}^{(N)} -$$
$$r_3\left(\theta_{j+1}^N - \theta_{j-1}^N\right)\left(U_{j+1}^N - U_{j-1}^N\right) + \Delta t Gr\theta_j^N + \Delta t GcC_j^N \tag{10}$$

$$-r_1C_{j-1}^{(N+1)} + (Sc+2r_1)C_j^{(N+1)} - r_1C_{j+1}^{(N+1)} = r_2C_{j-1}^{(N)} + (Sc-2r_2)C_j^{(N)} +$$
$$r_2C_{j+1}^{(N)} + r_5\left(\theta_{j-1}^N - 2\theta_j^N + \theta_{j+1}^N\right) \tag{11}$$

$$-r_1\theta_{j-1}^{(N+1)} + (\Pr+2r_1)\theta_j^{(N+1)} - r_1\theta_{j+1}^{(N+1)} = r_2\theta_{j-1}^{(N)} + (\Pr-2r_2 - S\Delta t)\theta_j^{(N)} + r_2\theta_{j+1}^{(N)} + \tag{12}$$
$$\lambda\Delta t\, \exp\left(\frac{\theta_j^{(N)}}{1+\varepsilon\theta_j^{(N)}}\right) + r_4\left(C_{j-1}^N - 2C_j^N + C_{j+1}^N\right)$$

where $r_1 = \xi\Delta t / \Delta y^2$, $r_2 = (1-\xi)\Delta t / \Delta y^2$, $r_3 = \mu X\Delta t / 4\Delta y^2$, $r_4 = Du\Pr\Delta t / \Delta y^2$, $r_5 = Sr\Delta t / \Delta y^2$ $\mu = 1 - X\theta$, and $0 \le \xi \le 1$. We chose $\xi = 1$ the detailed reasons to this particular selection is documented in [34].

4. RESULTS AND DISCUSSION

To study the behavior of the solutions, numerical calculations for some values of Frank-Kamenetskii parameter (λ), Soret number (Sr), Dufour number (Du), variable viscosity parameter (X), heat generating/absorbing parameter (S), Schmidt number (Sc), Prandtl number (Pr), thermal Grashof number (Gr), mass Grashof number (Gc), and non-dimensional time (t) have been carried out. Unless otherwise stated, the values: $\lambda = 0.1, X = 0.1$, Du = 0.01, $Gr = 0.1$, S = 0.1, $Gc = 0.1$, Sr = 0.1, $\theta_a = 1$, $C_a = 1$, Pr = 0.71, Sc = 0.62, $t = 0.1$ and $\varepsilon = 0.01$ are used for the investigation. Results obtained are displayed graphically for velocity, temperature, concentration, skin friction, Nusselt number and Sherwood number for various flow parameters.
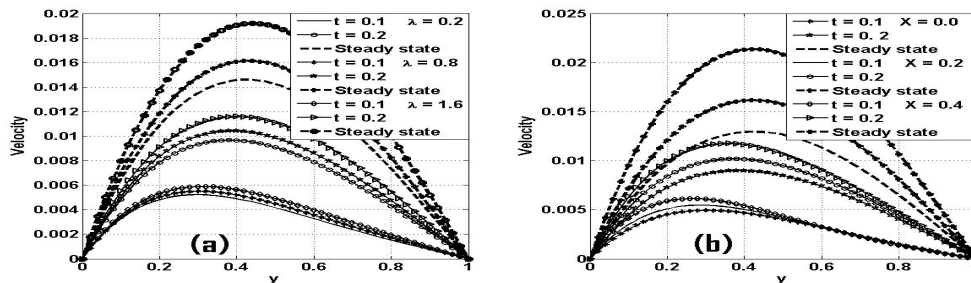

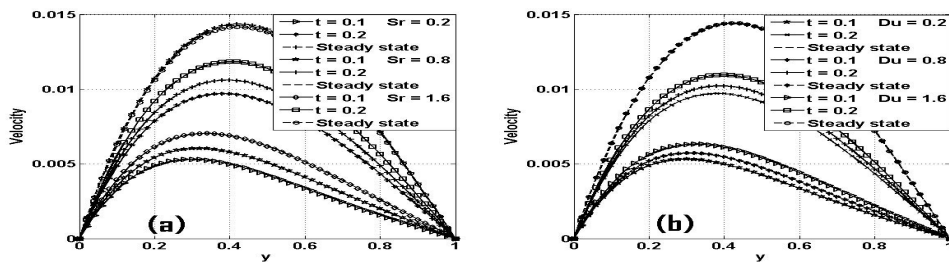Fig.2. Variation of unsteady and steady-state velocity with λ and X

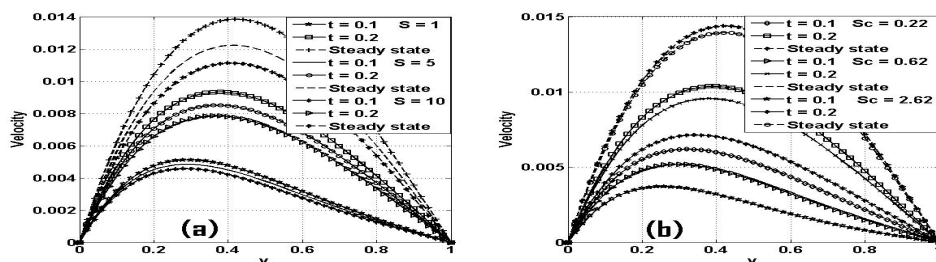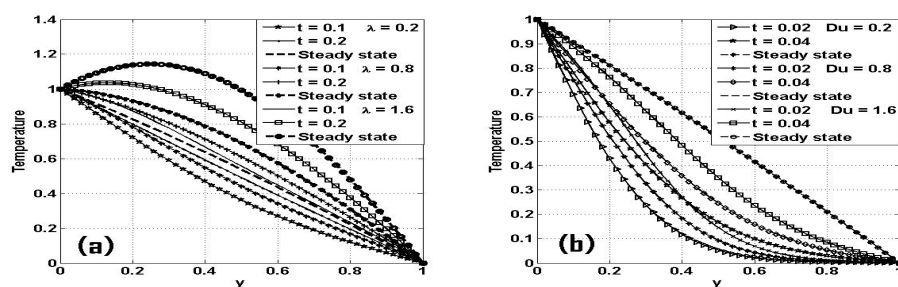Fig.3. Variation of unsteady and steady-state velocity with Sr and Du
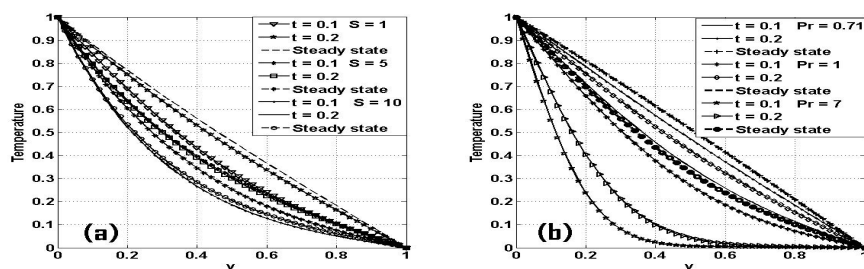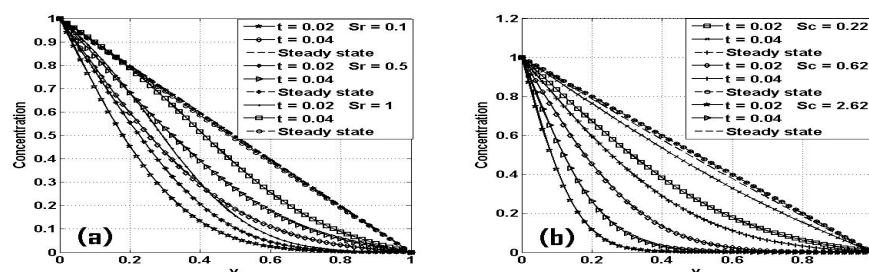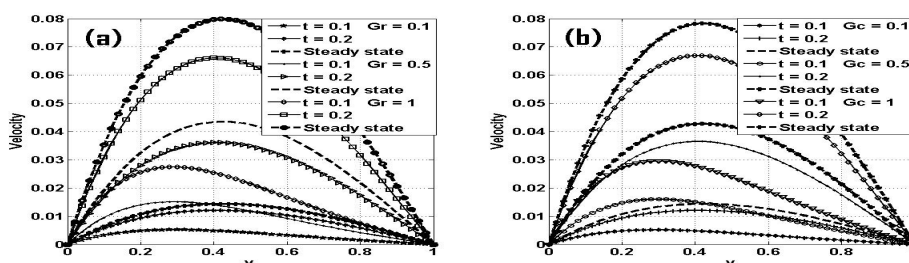

Fig.4. Variation of unsteady and steady-state velocity with S and Sc

Fig.5. Variation of unsteady and steady-state temperature with λ and Du

Fig.6. Variation of unsteady and steady-state temperature with S and Pr

Fig.7. Variation of unsteady and steady-state concentration with Sr and Sc

Fig.8. Variation of unsteady and steady-state velocity with Gr and Gc

In fig.2a, the effect of the Frank-Kamenetskii parameter (λ) and non-dimensional time (t) on velocity profiles is analyzed. From this figure it is observed that both unsteady and steady-state velocity of the fluid increases with increasing values of λ. This is physically true since an increase in λ lead to significant increases in the reaction and viscous heating source terms and hence considerably increases the fluid velocity. The influence of the variable viscosity parameter (X) and time (t) on the velocity profiles is illustrated in fig.2b. The graph shows that as X increases, the fluid becomes less viscous and hence their molecular resistance to motion decreases, and thereby increases in the fluid flow. It is also seen from fig.2b that the velocity of the fluid is maximum in the vicinity of the hot wall ($y = 0$) and then gradually decreases as it moves towards the cooled wall ($y = 1$). The response of the velocity variations in the thermal diffusion (Sr) and diffusion-thermo (Du) is illustrated in fig.3a and 3b respectively. Fig.3a and 3b revealed that an increase in Sr and Du accelerate the velocity of the fluid. In addition, as time increases, the velocity of the fluid also increases until a steady-state value is achieved. Fig.4a and 4b represent the velocity profiles for different values of heat sinks parameter (S) and Schmidt number (Sc) respectively. From fig.4a it is noted that velocity of the fluid decreases with increasing values of S. As expected, since increasing values of S results to the cooling of the fluid which leads to the decrease in the fluid

velocity. The values of Schmidt number (Sc) are chosen for hydrogen (Sc = 0.22), water vapor (Sc = 0.62) at temperature 25^{0}C and propylbenze (Sc = 2.62). In fig.4b, it is seen that small value of Sc increases both unsteady and steady-state velocity, while higher values of Sc decreases the velocity of the fluid.

The effect of the Frank-Kamenetskii parameter (λ) and diffusion-thermo (Du) on the temperature field is displayed in fig.5a and 5b respectively. An increase in λ cause an increase in the reaction and viscous heating source terms and in turn increase the fluid temperature see fig.5a. The diffusion-thermo (Du) represents the thermal energy flux in the flow. It is clear from fig.5b that an increase in Du causes a rise in the temperature of the fluid. Fig.6a and 6b show the influence of the heat sinks parameter (S) and Prandtl number (Pr) on the temperature field respectively. From fig.6a it is observed that temperature of the fluid decreases with increasing S. This is true since increasing S results to the cooling of the fluid which leads to the decrease in the temperature of the fluid. Larger values of the Prandtl number (Pr) correspondingly decrease the strength of the source terms in the temperature equation and hence in turn reduce the temperature as clearly illustrated in fig.6b. Fig.7a and 7b represent the concentration profiles for different values of Sr and Sc respectively. It is evident from fig.7a that increasing values of Sr increases the concentration of the fluid. Fig.7b revealed that small value of Sc increases fluid concentration while larger value of Sc reduces the concentration of the fluid. Fig.8a and 8b represent the velocity profiles for different values of the thermal Grashof number (Gr) and mass Grashof number (Gc) respectively. These plots fig.8a and 8b indicate that the momentum boundary layer thickness increases with increasing values of Gr and Gc. The consequence of the increased buoyancy source terms due to higher values of Gr and Gc increases both unsteady and steady-state velocity of the fluid.
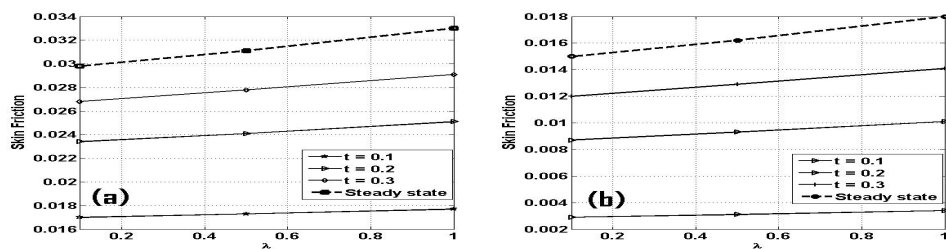

Fig.9. Variation of unsteady and steady state skin friction at $y = 0$ and $y = 1$ with λ
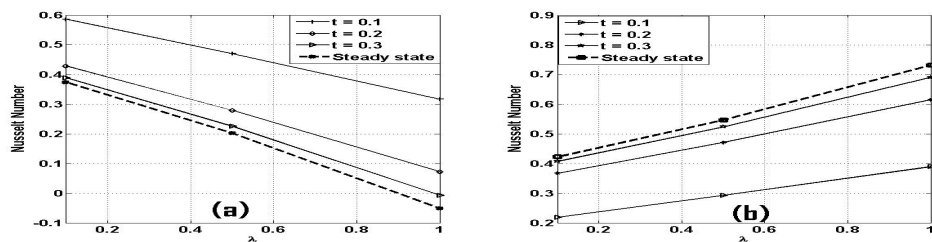

Fig.10. Variation of unsteady and steady state Nusselt number at $y = 0$ and $y = 1$ with λ
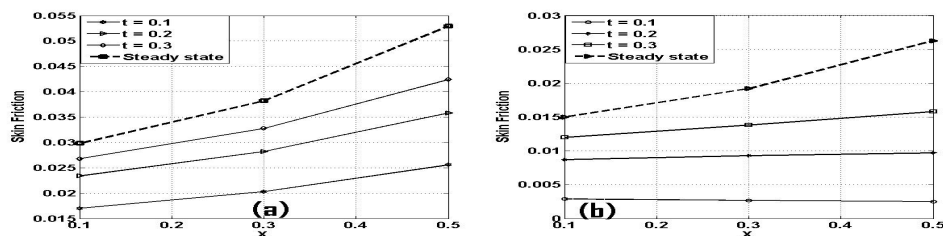

Fig.11. Variation of unsteady and steady state skin friction at $y = 0$ and $y = 1$ with X

The wall shear stress dependence on Frank-Kamenetskii parameter (λ) for varying values of time (t) at the plate $y = 0$ and $y = 1$ is illustrated in fig.9a and 9b respectively. From fig.9a and 9b it can be noticed that skin friction increases with increasing both λ and t until a steady-state condition is achieved. Fig.10a and 10b are plotted to see the effect of λ and t on the rate of heat

transfer (Nusselt number) at the plate $y = 0$ and $y = 1$ respectively. Fig.10b reveals that the rate of heat transfer increases as λ and t increases until a steady-state condition is attained. A reverse effect is observed at the plate $y = 0$ see fig.10a.
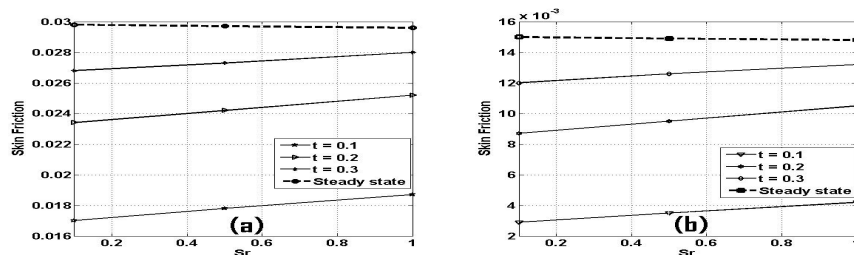

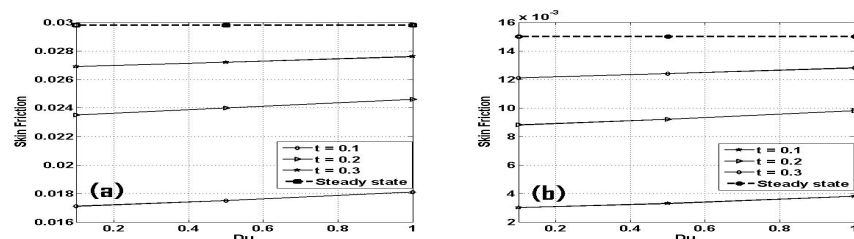Fig.12. Variation of unsteady and steady state skin friction at $y = 0$ and $y = 1$ with Sr

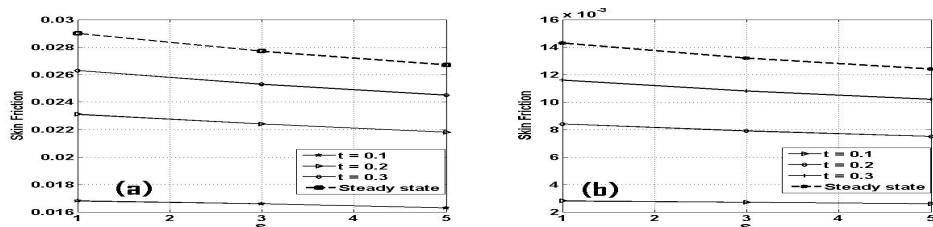Fig.13. Variation of unsteady and steady state skin friction at $y = 0$ and $y = 1$ with Du

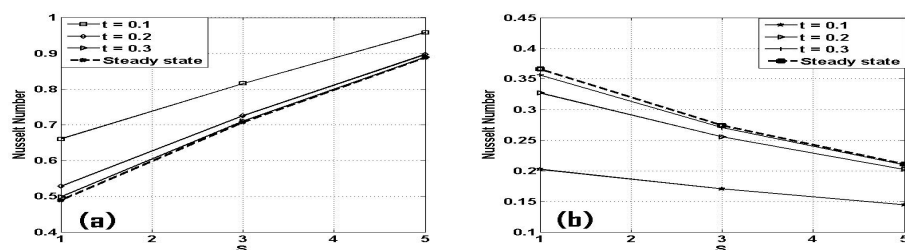Fig.14. Variation of unsteady and steady state skin friction at $y = 0$ and $y = 1$ with S

Fig.15. Variation of unsteady and steady state Nusselt number at $y = 0$ and $y = 1$ with S
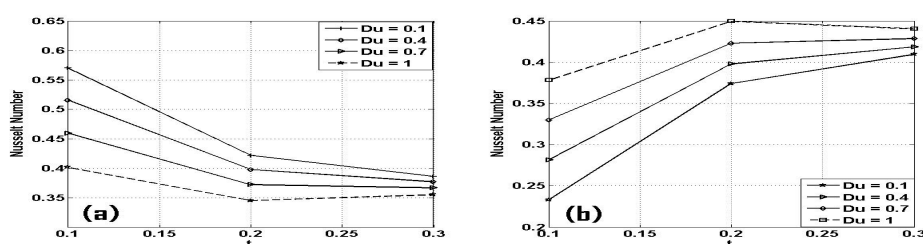

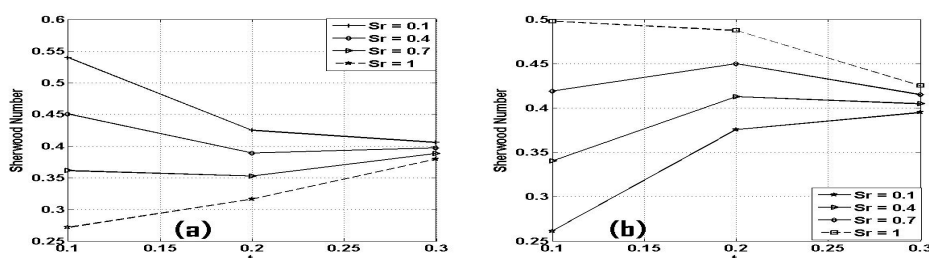Fig.16. Variation of Nusselt number at $y = 0$ and $y = 1$ with Du and t

Fig.17. Variation of Sherwood number at $y = 0$ and $y = 1$ with Sr and t

The skin friction dependence on variable viscosity parameter (X) for varying values of time (t) at the plate $y = 0$ and $y = 1$ is illustrated in fig.11a and 11b respectively. These figures reflected that skin friction increases with increasing X and t until a steady-state condition is reached. Figs.12 and 13 represent the skin friction dependence on Sr and Du for varying values of time respectively. It is clear from these plots that skin friction increases as Sr and Du increases. It is also noticed that as t increases, the skin friction increases until a steady-state value is achieved.
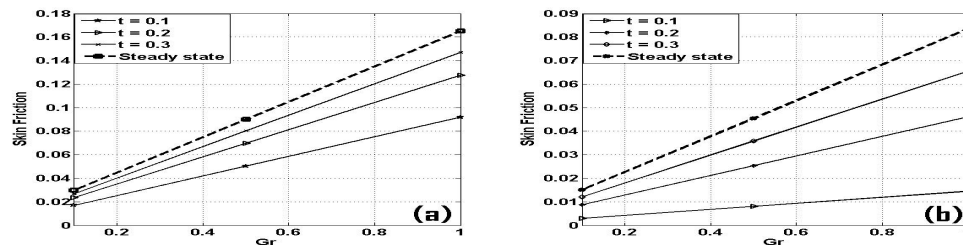

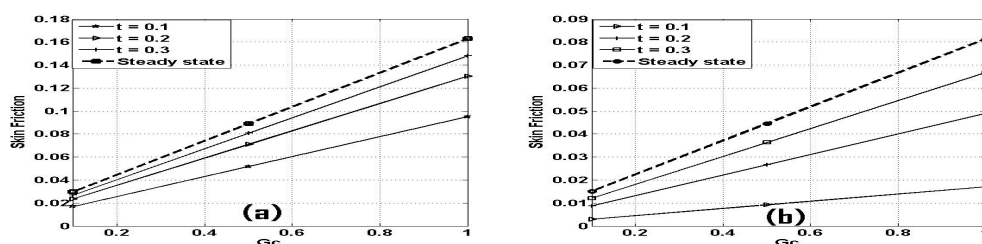Fig.18. Variation of unsteady and steady state skin friction at $y = 0$ and $y = 1$ with Gr

Fig.19. Variation of unsteady and steady state skin friction at $y = 0$ and $y = 1$ with Gc

Figs.14 and 15 illustrated the wall shear stress and Nusselt number dependence of heat sinks parameter (S) for varying values of time (t). It is seen from fig.14 that skin friction slightly decreases with increasing values of S and t at the plate $y = 0$ and $y = 1$ until a steady-state is reached. In fig.15b it is observed that rate of heat transfer at the wall $y = 1$ decreases with increasing values of S and t. A similar effect is observed but in opposite direction at the plate $y = 0$ sees fig.15a.

The rate of heat transfer (Nusselt number) dependence on time (t) at the plate $y = 0$ and $y = 1$ is depicted in fig.16a and 16b respectively for varying values of Du. It is clearly seen from fig.16a that Nusselt number decreases as Du and t increase. Similar trend is observed but in opposite direction at the plate $y = 1$ sees fig.16a. The rate of mass transfer (Sherwood number) dependence on t at the plate $y = 0$ and $y = 1$ is displayed in fig.17a and 17b respectively for varying values of Sr. Fig.17a reveals that the rate of mass transfer decreases due to the increase in Sr and time. A similar trend is noticed but in opposite direction at the plate $y = 1$ sees fig.17b. Figs.18 and 19 show the wall shear stress dependence on Gr and Gc for varying values of t respectively. From these figures it is noticed that as time increase, the frictional force due to the motion of the fluid also increases until a steady-state condition is attained. Figs.18 and 19 reflected that values of Gr and Gr increase the skin friction.

5. CONCLUSION

In this paper, the problem of unsteady as well as steady flow of viscous reactive, heat generating/absorbing fluid between two infinite vertical walls in the presence of thermal diffusion, diffusion-thermo and temperature dependent variable viscosity was investigated numerically using unconditionally stable and convergent semi-implicit finite difference scheme. It is found that thermal diffusion, diffusion-thermo, non-dimensional time and temperature dependent variable viscosity accelerate fluid flow while heat sinks reduce the motion of the fluid.

References

[1.] A. C. Campbell, S.S.S. Cardoso, A.N. Hayhurst, A comparison of measured temperatures with those calculated numerically and analytically for an exothermic chemical reaction inside a spherical batch reactor with natural convection, Chem. Eng. Sci., 62(2007) 3068-3082.

[2.] E.R.G. Eckert, R.M. Drake, *Analysis of Heat and Mass Transfer*, McGraw-Hill, New York (1972).

[3.] E.M. Sparrow, W.J. Minkowyez, E.R.G. Eckert, Effects of diffusion thermo and thermal diffusion on heat transfer, flow and mass transfer for the helium-air boundary layer in stagnation flow, ASME J. Heat Transfer, 86C (1964) 508-512.

[4.] T. Hayat, M. Mustafa, I. Pop, Heat and mass transfer for Soret and Dufour's effect on mixed convection boundary layer flow over a stretching vertical surface in a porous medium filled with a visco-elastic fluid, Commun. Nonlinear Sci.Numer.Simulat. 15 (2010) 1183-1196.

[5.] M.S. Alam, M.M. Rahman, Dufour and Soret effects on mixed convection flow past a vertical porous flat plate with variable suction, Nonlinear Analysis: Modelling and Control, 11 (2006) 3-12.

[6.] C.Y. Cheng, Soret and Dufour effects on natural convection boundary layer flow over a vertical cone in a porous medium with constant wall heat and mass fluxes, Int. Commun. Heat and Mass Transfer, 38 (2011) 44-48.

[7.] R. Tsai, J.S Huang, Numerical study of Soret and Dufour effects on heat and mass transfer from natural convection from over a vertical porous medium with variable wall heat fluxes, Computational Materials Sci., 47 (2009) 23-30.

[8.] R. Tsai, J.S. Huang, Heat and mass transfer for Soret and Dufour's effects on Hiemenz flow through porous medium onto a stretching surface, Int. J. of Heat and Mass Transfer, 52 (2009) 2399-2406.

[9.] M. Eugen, A. Postelnicu, Double-diffusive natural convection flows with thermosolutal symmetry in porous media in the presence of the Soret-Dufour effects, Transport in Porous media, 88 (2011) 149-167.

[10.] A. Postelnicu, Influence of a magnetic field on heat and mass transfer by natural convection from vertical surfaces in porous media considering Soret and Dufour effects, Int. J. of Heat and Mass Transfer, 47 (2004) 1467-1472.

[11.] S.T. Shyam, M. Rajeev, K.G. Rohit, K. Aiyub, MHD free convection-radiation interaction along a vertical surface embedded in Darcian porous medium in the presence of Soret and Dufour effects, Thermal Sci., 14 (2010) 137-145.

[12.] P.O. Olanrewaju, O.J. Fenuga, J.A. Gbadeyan, T.G. Okedayo, Dufour and Soret effects on convection heat and mass transfer in an electrically conducting power law flow over a heated porous plate, Int. J. Computational Methods, 14 (2013) 32-39.

[13.] M.G. Reddy, N.B. Reddy, Soret and Dufour effects on steady MHD free convection flow past a semi-infinite moving vertical plate in a porous medium with viscous dissipation, Int. J. of Appl. Math and Mech., 6 (2010) 1-12.

[14.] A.A. Afify, Similarity solution in MHD effects of thermal diffusion and diffusion thermo on free convective heat and mass transfer over a stretching surface considering suction or injection, Commun. Nonlinear Sci. Numer.Simulat., 14 (2009) 2202-2214.

[15.] A. Mahdy, MHD non-Darcian free convection from a vertical wavy surface embedded in porous media in the presence of Soret and Dufour effect, Int. Commun. Heat and Mass transfer, 36 (2009) 1067-1074.

[16.] E. Osalusi, J. Side, R. Harris, Thermal diffusion and diffusion-thermo effects on combined heat and mass transfer of a steady MHD convective and slip flow due to a rotating disk with viscous dissipation and ohmic heating, Int. Commun. Heat and Mass Transfer, 35 (2008) 908-915.

[17.] M.S. Alam, M.M. Rahman, A. Maleque, M. Ferdows, Dufour and Soret effects on steady MHD combined free-forced convective and mass transfer flow past a semi-infinite vertical plate, Thammasat Int. J. Sci. and Techn., 11 (2006) 1-12.

[18.] A.J. Chamkha, A. Ben-Nakhi, MHD mixed convection-radiation interaction along a permeable surface immersed in a porous medium in the presence of Soret and Dufour effects, Heat Mass Transfer, 44 (2008) 845-856.

[19.] A. Postelnicu, Influence of chemical reaction on heat and mass transfer by natural convection from vertical surfaces in porous media considering Soret and Dufour effects, Heat Mass Transfer, 43 (2007) 595-602.

[20.] M.A. Mansour, N.F. El-Anssary, A.M. Aly, Effects of chemical reaction and thermal stratification on MHD free convective heat and mass transfer over a vertical stretching surface embedded in a porous media considering Soret and Dufour numbers, J. chemical Eng., 145 (2008) 340-345.

[21.] O.A. Beg, T.A. Beg, A.Y. Bakier, V.R. Prasad, Chemically-reacting mixed convective heat and mass transfer along inclined and vertical plates with Soret and Dufour effects: Numerical solutions, Int. J. of Appl. Math and Mech., 5 (2009) 39-57.

[22.] S.M.M. El-Kabeir, A. Chamkha, A.M. Rashad, Heat and mass transfer by MHD stagnation-point flow of a power-law fluid towards a stretching surface with radiation, chemical reaction and Soret and Dufour effects, Int. J. Chemical Reactor Eng., 8 (2010) 1-18.

[23.] K. Gangadhar, Soret and Dufour effects on hydromagnetic heat and mass transfer over a vertical plate with a convective surface boundary condition and chemical reaction, J. Appl. Fluid Mech., 6 (2013) 95-105.

[24.] R. Bhargava, R. Sharma, O.A. Beg, Oscillatory chemically-reacting MHD free convection heat and mass transfer in a porous medium with Soret and Dufour effects: Finite element modeling, Int. J. of Appl. Math. Mech., 5 (2009) 15-37.

[25.] D. Pal, H. Mondal, Effects of Soret Dufour, chemical reaction and thermal radiation on MHD non-Darcy unsteady mixed convective heat and mass transfer over a stretching sheet, Commun. Nonlinear Sci. Numer Simulat, 16 (2011) 1942-1958.

[26.] S.R. Vempati, A.B. Laxmi-Narayana-Gari, Soret and Dufour effects on unsteady MHD flow past an infinite vertical porous plate with thermal radiation, Appl. Math. Mech., 31 (2010) 1481-1496.

[27.] M.Q. Al-Odat, A. Al-Ghamdi, Numerical investigation of Dufour and Soret effects on unsteady MHD natural convection flow past vertical plate embedded in non-Darcy porous medium, Appl. Math. Mech., 33 (2012) 195-210.

[28.] M.A. Hossain, K. Khanafer, K. Vafai, The effect of radiation on free convection flow of fluid with variable viscosity from a porous vertical plate, Int. J. Thermal Sci., 40 (2001) 115-124.

[29.] N.G. Kafoussias, E.W. Willians, Thermal diffusion and diffusion-thermo effects on mixed free-forced convective and mass transfer boundary layer flow with temperature dependent viscosity, Int. J. Engng. Sci., 33 (1995) 1369-1384.

[30.] M.A. Seddeek, Thermal-diffusion and diffusion-thermo effects on mixed free-forced convective flow and mass transfer with a heat source in the presence of suction and blowing in the case of variable viscosity, Acta Mechanica, 172 (2004) 83-94.

[31.] M.B.K. Moorthy, K. Senthilvadivu, Soret and Dufour effects on natural convection flow past a vertical surface in a porous medium with variable viscosity, J. Appl. Mathematics, Article I.D 634806, (2012) 1-15.

[32.] B.K. Jha, A.O. Ajibade, Free convective flow of heat generating/absorbing fluids between vertical porous plates with periodic heat input, Int. Commun. Heat Mass Transfer, 36(2009) 624-631.

[33.] I.A. Abdullah, Analytic solution of heat and mass transfer over a permeable stretching plate affected by chemical reaction, internal heating, Dufour-Soret effect and hall effect, Thermal Sci., 13 (2009) 183-197.

[34.] O.D. Makinde, T. Chinyoka, Numerical study of unsteady hydromagnetic generalized Couette flow of a reactive third-grade fluid with asymmetric convective cooling. Computers and Math. Appl., 61 (2011) 1167-1179.

ANNALS of Faculty Engineering Hunedoara – International Journal of Engineering